Colloids and Surfaces A: Physicochemical and Engineering Aspects 686 (2024) 133468

Contents lists available at ScienceDirect

Colloids and Surfaces A: Physicochemical and Engineering Aspects

journal homepage: www.elsevier.com/locate/colsurfa

Magnetic field-dependent dynamic behavior of magnetorheological grease composite in a wide temperature range: Experiment and modeling

Huixing Wang [a], Shuna Xue [a], Kun Qian [a], Yancheng Li [b,*], Jiong Wang [a]

[a] School of Mechanical Engineering, Nanjing University of Science and Technology, Nanjing 210094, People's Republic of China
[b] School of Civil and Environmental Engineering, University of Technology Sydney Ultimo 2007, Australia

GRAPHICAL ABSTRACT

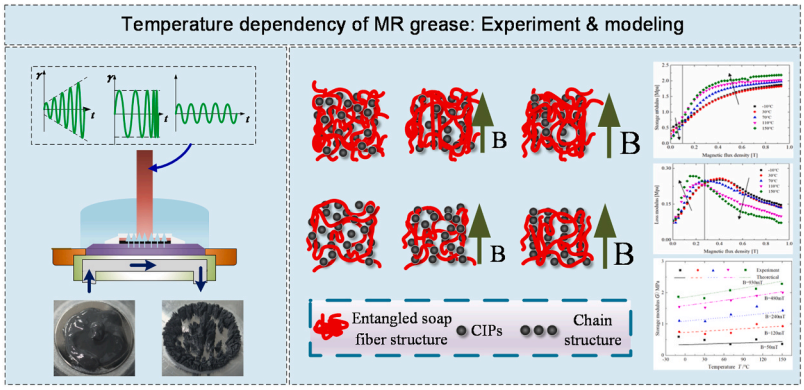

ARTICLE INFO

Keywords:
MR grease
Dynamic behavior
Wide temperature range
Model

ABSTRACT

Investigating the intricate magneto-induced dynamic behavior of Magnetorheological (MR) grease is a prerequisite for the design of its devices. This paper is mainly concerned with comprehensive experimental and modeling research of the magneto-induced dynamic characteristics over a wide temperature range. Firstly, a lab-prepared lubricant grease matrix was used to produce a MR grease that exhibits as soft matter under zero field condition, and its magneto-induced dynamic shear properties under the temperature range of −10°C to 150°C was tested by three types of experiments, i.e., oscillatory strain amplitude, oscillatory frequency and magnetic field sweeps. Secondly, the temperature dependent dynamic behavior of MR grease, i.e., stress-strain hysteresis characteristics and storage/loss modulus variation, under different strain amplitudes, frequencies and magnetic fields is discussed and analyzed in detail. The variation of the stress-strain hysteresis suggests that MR grease exhibits thermal-softening effect in the absence of magnetic field, while it demonstrates thermo-stiffening in the presence of magnetic field. The study of storage/loss modulus reveals a pronounced sensitivity to variations in magnetic field, temperature, and strain magnitude, with the exception of oscillation frequency, which exhibits relatively lower sensitivity. Furthermore, within the linear viscoelastic range, both storage modulus and loss modulus are associated with the critical magnetic field, leading to a response that is completely opposite across the temperature range from −10°C to 150°C. Finally, a model consisting of a five-parameter viscoelastic element

* Corresponding author.
E-mail address: yancheng.li@uts.edu.au (Y. Li).

https://doi.org/10.1016/j.colsurfa.2024.133468
Received 4 December 2023; Received in revised form 25 January 2024; Accepted 8 February 2024
Available online 10 February 2024
0927-7757/© 2024 The Author(s). Published by Elsevier B.V. This is an open access article under the CC BY-NC-ND license (http://creativecommons.org/licenses/by-nc-nd/4.0/).

and Arrhenius equation was proposed to predict the magnetic field- and temperature-dependent storage/loss modulus of MR grease under different oscillatory strain amplitudes and frequencies, and the effectiveness of the model was verified by comparing experimental and simulated results.

1. Introduction

Multifunctional composite materials, due to their ability to change their characteristics in response to external stimuli, are driving a major transformation in the field of engineering [1]. Of great interest are MR smart materials that react to magnetic fields, as they allow for reversible control of damping and stiffness [2–4]. MR grease composite is a type of MR smart material, usually fabricated by incorporating magnetic particles into a lubricant grease matrix [3,5,6]. The macroscopic behavior of MR grease can be adjusted from a liquid to a soft state by controlling the weight fraction of thickening agents in the grease matrix. When the concentration of thickening agents in the grease matrix is low, MR grease exhibits similarities to MR fluid with a traditional silicon oil-based matrix. However, due to the entanglement of soap fibers in the grease, MR grease possess improved sedimentation characteristics compared to MR fluid [6,7]. With the increase of thickening agent content, it presents a soft state in the absence of a magnetic field, somewhat similar to MR elastomer. However, in contrast to MR elastomer, where iron particles are unable to move within the elastomer matrix, iron particles in MR grease can still be arranged into chains-like structure under magnetic fields, resulting in a higher MR effect compared to MR elastomer [5,7]. Therefore, the development of MR grease presents a new possibility for engineering applications, such as dampers [8–10], isolators [11–14], sensors [15,16], and actuators [17–19].

As known, in a substantial number of engineering applications for MR materials, the performance of the devices usually depends on the dynamic shear properties of the material under various stimuli.

Currently, research on the dynamic rheological behavior of MR materials is mostly concentrated on Magnetic nanofluids, MR fluids and MR elastomer, and the commonly used research method is oscillatory shear testing [3,20–22]. Oscillatory methods typically include strain amplitude sweep and frequency sweep [21,23]. In the strain amplitude sweep, when the shear strain is within the linear viscoelastic region, the storage modulus and loss modulus exhibit different dependence on the magnetic field strength at low, medium, and high magnetic fields. Moreover, the linear viscoelastic region continuously decreases with increasing magnetic field strength [21,23,24]. In frequency sweep studies, different experiments and simulations indicate that the moduli of a system can exhibit constancy, reach a maximum, or undergo either a decrease or an increase, depending on the specific characteristics of the system being investigated [21,25]. In the construction of dynamic behavior models, the theory based on the magnetic dipole interaction between adjacent particles within particle chains has been extensively employed [26]. In all, researchers have achieved a relatively mature understanding of the dynamic characteristics of MR fluids in current studies.

However, the soap-fiber microstructure of the grease matrix utilized in MR grease confers distinctive characteristics that diverge from those of conventional MR fluids and MR elastomers. Consequently, there has been a proliferation of studies exploring the dynamic behavior of MR grease under oscillatory shear with different loading conditions. Mohamad et al. conducted a series of studies to examine the influence of magnetic field on the storage and loss modulus for different MR grease samples under various oscillatory shear amplitudes and frequencies [3,27,28]. The results indicated that the maximum relative MR effect of the MR grease was determined to be 952.38%. Furthermore, the viscosity and storage modulus of MR grease increase with the increase of the magnetic field, and Payne's effect is observed at strains above 0.1% under magnetic field conditions which limits the LVE range of MR grease. Tarmizi et al. prepared two MR greases with different cobalt-ferrite particle concentrations and carried out experimental investigations on their linear viscoelastic range under varying magnetic fields and loading frequencies [29]. The results demonstrated that the utilization of CoFe2O4 in the MRG is able to enlarge the LVE range and enhanced the storage modulus and the absolute MR effect. Wang et al. investigated the nonlinear dynamic behavior of MR grease under lager oscillatory shear by using Fourier transform (FT)-Chebyshev analysis and found that MRG-70 exhibits the nonlinearities with different combination of strain stiffening and shear thinning [30]. It showed that intracycle elastic nonlinearity are more affected by the magnetic field than the intracycle viscous nonlinearity. However, compared to intercycle viscous nonlinearity, the intercycle elastic nonlinearity seems to be less affected by the magnetic field.

To examine the dynamic shear behavior of MR grease, in addition to the common excitations, i.e., magnetic field and oscillation frequency and strain amplitude, the influence of temperature arose from the environmental or working conditions cannot be disregarded as a relevant consideration. Especially for MR grease, the entangled soap fiber structure of the internal grease matrix is coupled with the magneto-induced chain structures, and this coupling behavior becomes more complex when the temperature changes [3,4]. Thus, the study on dynamic characteristics of MR grease with a focus on the temperature factor has been paid increasing attention in recent years. Pan et al. explored the rheological characteristics and thermal-magnetic coupling mechanism of MR grease within the 20℃ to 80℃ temperature range [31]. Ye et al. examined the dynamic hysteresis behavior of MR grease when the temperature increase from 10℃ to 90℃, and found that the elastic and viscous properties decreased with the increase in temperature [32,33]. Wang et al. performed experiments to examine the alteration in the storage and loss moduli of MR grease over the temperature range from 10℃ to 70℃. The results discovered that the rheological changes of MR grease at different temperatures are greatly influenced by the microstructure of the grease matrix [5].

The aforementioned works have explored temperature influence on the performance of MR grease. However, it is noteworthy that the temperature range is almost exclusively restricted within 10°C to 90°C. In reality, the working temperature of MR devices can often exceed 100°C or drop below 0°C, such as in a vehicle suspension. Aside from the limited temperature loading conditions, the aforementioned research have largely centered around experimental characterization, with limited attention being paid to the development of predictive models for the temperature-dependent dynamic response of MR grease under various excitations, e.g., magnetic fields or oscillation frequencies. The availability of validated models would be highly beneficial, as they would obviate the requirement for extensive and costly experimental validation procedures, and would also provide a valuable resource for design optimization purposes. Consequently, it is imperative to undertake experimental investigations that span a wider temperature range to better comprehend the dynamic characteristics of MR grease, and establish predictive models that accurately capture these behaviors. In this work, A lab-prepared lubricant grease matrix was used to produce a MR grease that exhibits a soft matter state under zero field conditions. Then three distinct varieties of oscillatory shear experiments, i.e., strain amplitude sweep (from 0.01% to 10%), frequency sweep (from 0.1 Hz to 100 Hz) and magnetic field sweep (from 0 to 1 T) at fixed strain amplitude (0.01%) and frequency(1 Hz), were conducted across a broad temperature spectrum (from −10℃ to 150℃) to explore the temperature-dependent dynamic characteristics of MR grease. The temperature dependent magneto-induced characteristics of stress-strain

hysteresis loop and storage/loss moduli under different oscillatory strain amplitudes and frequencies are discussed and analyzed in detail. Finally, a model consisting of a five-parameter viscoelastic element and Arrhenius equation is proposed to describe the temperature dependence dynamic of MR grease.

2. Fabrication of MRG sample

The MR grease composite was prepared through the dispensation of ferromagnetic particles into the grease matrix. In existing literature, the lubricating grease base is typically obtained directly from the market [3,31,34]. However, the fixed NIGL grade of such grease base may prove inadequate to meet the complex demands of engineering applications on zero-field viscosity or stiffness. To overcome aforementioned limitation, a composite lithium-based grease matrix was synthesized by utilizing a saponification reaction. The advantage of this method lies in the ability to obtain grease matrix with varying degrees of softness and hardness by adjusting the ratio of thickener and base oil content or the viscosity of the base oil.

Fig. 1(a) shows the preparation process of the MR grease composite with 70% weight fraction of carbonyl iron particles (CIPs), which mainly includes four steps.

Step 1: Add 12-hydroxystearic acid and sebacic acid into silicone oil, and then heat to 80–100 ℃ while mechanically stirring for 30 minutes.

Step 2: Add lithium hydroxide into the beaker and maintain the saponification reaction for 2 hours.

Step 3: Add diphenylamine into the beaker, heat up to 130–140 ℃ and dehydrate for 30 minutes.

Step 4: Add CIPs into the grease matrix, raise the temperature to 150–180 °C, and perform a 45-minute low-temperature thickening process. Then, further raise the temperature to 180–200 °C and perform a 15-minute high-temperature thickening process. Finally, cool and stir until it reaches room temperature.

Table 1 shows the details and amount of the experimental ingredients used in the above steps. Table 2 shows the elemental analysis of the CIP along with its particle size distribution. The specific surface area determined by BET method is 0.7 m^2/g. The moisture content is test by the C30S provided by METTLER based on Karl Fischer method, and the results showed a water content of the grease matrix approximately 0.0136%.

Table 1
Specific information of experimental ingredients.

Ingredients	Types	Manufacturer	Purity	Weight used
12-hydroxystearic acid	H-00994	Tianjin Heowns Biochem Technologies, LLC.	75%	4.41 g
sebacic acid	S-00200	Tianjin Heowns Biochem Technologies, LLC	98%	1.42 g
silicone oil	PMX-200	Dow Corning Silicone Co., Ltd.	/	113.4 g
lithium hydroxide	P02315	Shanghai Dingfen Chemical Technology Co., Ltd.	/	1.21 g
diphenylamine	M03782	Shanghai Myrell Chemical Technology Co., Ltd.	99%	0.6 g
CIPs	CN	BASF (china) Co., Ltd, Shanghai	99.5%	280 g

Table 2
Elemental analysis and particle size distribution of the CIP.

Particle size distribution	iron content (%)	Carbon content (%)	nitrogen content (%)	oxygen content (%)
Unit： um ×**10** <3.5 ×**50** <6 ×**90** <21	99.7	0.01	0.02	0.2

Fig. 1(b) shows a comparison of the magnetization curves between the prepared MR grease and pure CIPs. As can be seen from the figure, the saturation magnetic field strength of the MR grease is around 380 kA/m, while that of the pure CIPs is around 500 kA/m. The SEM

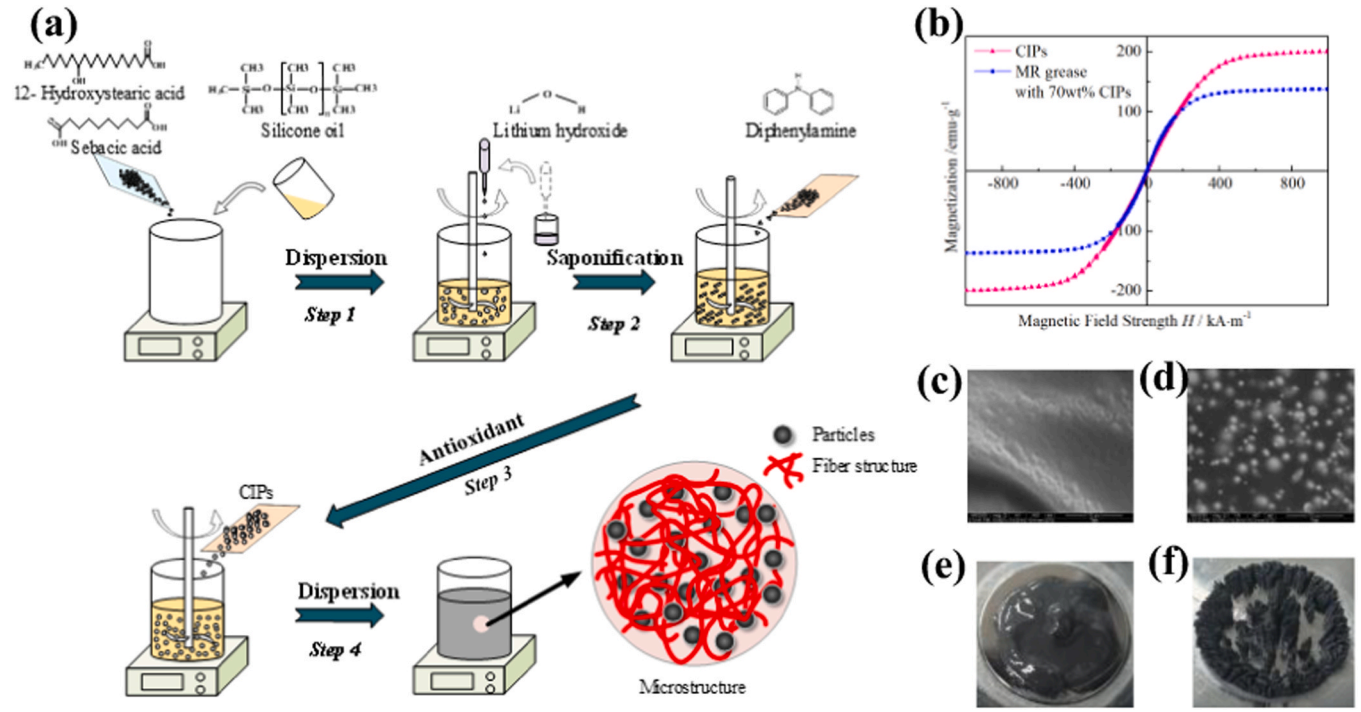

Fig. 1. Schematic diagram of the preparation process of MR grease (a); Magnetization curve of CIPs and MR grease (b); SEM images of grease matrix (c) and MR grease (d); Pictures of MR grease without magnetic field (e) and with magnetic field (f).

images of grease matrix and MR grease is shown in Fig. 1(c) and (d), respectively. Due to the nature of the base oil, the soap fiber structure is not visible in Fig. 1(c), and in Fig. 1(d), the CIPs are uniformly dispersed in the grease matrix. Fig. 1(e) and (f) shows the macroscopic behavior of MR grease under no magnetic field and with a magnetic field, respectively. When the magnetic field is not applied, the MR grease exhibits a soft state, while under a magnetic field, it transforms into cluster-like structure.

3. Experimental setup

The Schematic diagram for testing the dynamic performance of MR grease over a wide temperature range is presented by figure S1(a) in supporting information (SI). Figure S1(a) shows the testing host, and its schematic diagram is shown in Figure S1 (b). To conduct the experiment over a wider temperature range, the conventional water bath temperature control was replaced with an oil bath, and an insulating cover was used to avoid uneven temperature distribution in the sample. The heated or cooled oil is circulated through a closed loop to provide temperature control to the lower measuring plate, which in turn transfer to the MR grease sample. An insulating cover is utilized to maintain temperature consistency around the MR grease sample. A series of carefully-selected oscillatory shear loads, i.e., strain amplitude sweep (Figure S1 (c)), frequency sweep (Figure S1 (d)) and fixed amplitude and frequency (Figure S1 (e)), are applied to the sample on the upper measuring plate under the control of a driving motor. For MR testing systems with magnetic fields, the temperature control can be achieved within the range of −10 ℃ to 150℃.

In the testing process, the MR grease sample was consistently placed on the lower plate with a diameter of 20 mm, and the testing gap was maintained to be 1 mm. Upon regulated the MR grease sample to reach targeted temperatures, three types of tests were deployed to characterize the dynamic shear behavior of MR grease, i.e., strain amplitude sweep (Figure S1 (c)), frequency sweep (Figure S1 (d)) and fixed amplitude and frequency (Figure S1 (e)). In the first series of experiments, the sinusoidal strain amplitude increased logarithmically from 0.01% to 100%, with the frequency remaining constant at 1 Hz. The second test involved a logarithmic increase in the sinusoidal oscillation frequency from 0.1 Hz to 100 Hz, with the strain amplitude remaining constant at 0.01%. For each strain and frequency test, measurements were also taken at four levels of magnetic fields, i.e., 0mT, 120mT, 240mT and 480mT. In the final series, a magnetic field sweep experiment was conducted with a fixed strain amplitude and frequency, i.e., 0.01% and 1 Hz, where the magnetic field linearly increased from 0 mT to 920 mT. Each of the three types of tests was carried out at five different temperatures, namely −10 °C, 30°C, 70°C, 110°C and 150°C. Besides the commonly utilized values such as storage modulus and loss modulus, the raw stress-strain data from the tests were also extracted using the LAOS software that came with the Anton Paar MCR302.

4. Results and discussion

4.1. Static and dynamic yield stress

Fig. 2 illustrates the variation of static and dynamic yield stress with temperature under different magnetic field strengths. The detailed calculation process for static and dynamic yield stress is provided in the supplementary information. It can be observed that the trends of static and dynamic yield stress changes are similar. Regardless of the presence or absence of a magnetic field, both static and dynamic yield stress decrease with increasing temperature, which differs from the temperature dependence observed in the previously mentioned storage modulus and loss modulus. With the increase in magnetic field, the temperature dependence of static and dynamic yield stress seems to decrease continuously, exhibiting a similar characteristic to the aforementioned storage modulus and loss modulus.

For the static yield stress, i.e., τ, dependence on magnetic field, i.e., B, of MR materials, a function $\tau \propto H^b$ is widely employed, where b is the coefficient associate with the materials types and magnetic field. Philip et al. found in their study that within the range of 0–350 mT, the coefficient b for ferrofluids typically falls between 1 and 2 [20,21]. Ginder et al. discovered that for MR fluids, at lower magnetic field intensities, the yield stress is generally proportional to the square of the magnetic field strength, i.e., $\tau \propto H^2$, while under moderate magnetic field conditions, i.e., $\tau \propto H^{1.5}$, the yield stress exhibits a quadratic relationship with the magnetic field strength [24]. In the scope of our study on the MR grease, the static yield stress exhibits dependency on the magnetic field with coefficients of approximately 1.8 and 0.8, respectively, with 240 mT serving as the critical point. This can be attributed to the coupling between the soap fiber structure and the chain formation of magnetic particles.

4.2. Temperature dependent magneto-dynamic behavior under various strain amplitude

Fig. 3(a)-(d) illustrate the effect of temperature on the stress-strain hysteresis loops of MR grease which were measured under the small and lager strain amplitudes, i.e.,0.011% and 1%, with and without magnetic field, i.e.,0mT and 480mT. The frequency was maintained at 1 Hz. Regardless of temperature changes, the hysteresis loop of MR grease under small strain amplitude, i.e.,0.011%, always exhibits an elliptical shape, indicating linear viscoelastic behavior. Under the large shear strain of 1%, the hysteresis loop undergoes a twisting phenomenon, indicating nonlinear viscoelastic behavior. This suggests that, at a

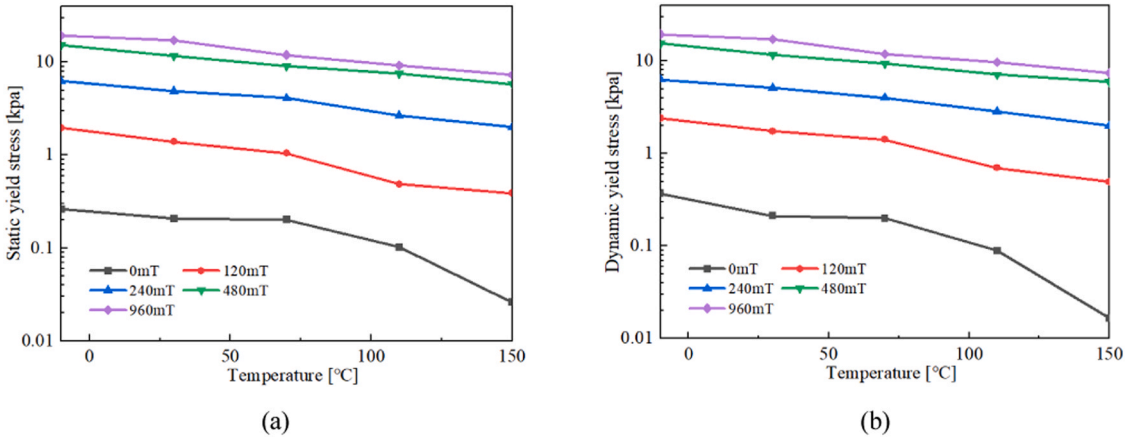

Fig. 2. Static yield stress (a) and dynamic yield stress (b) as a function of temperature under different magnetic field.

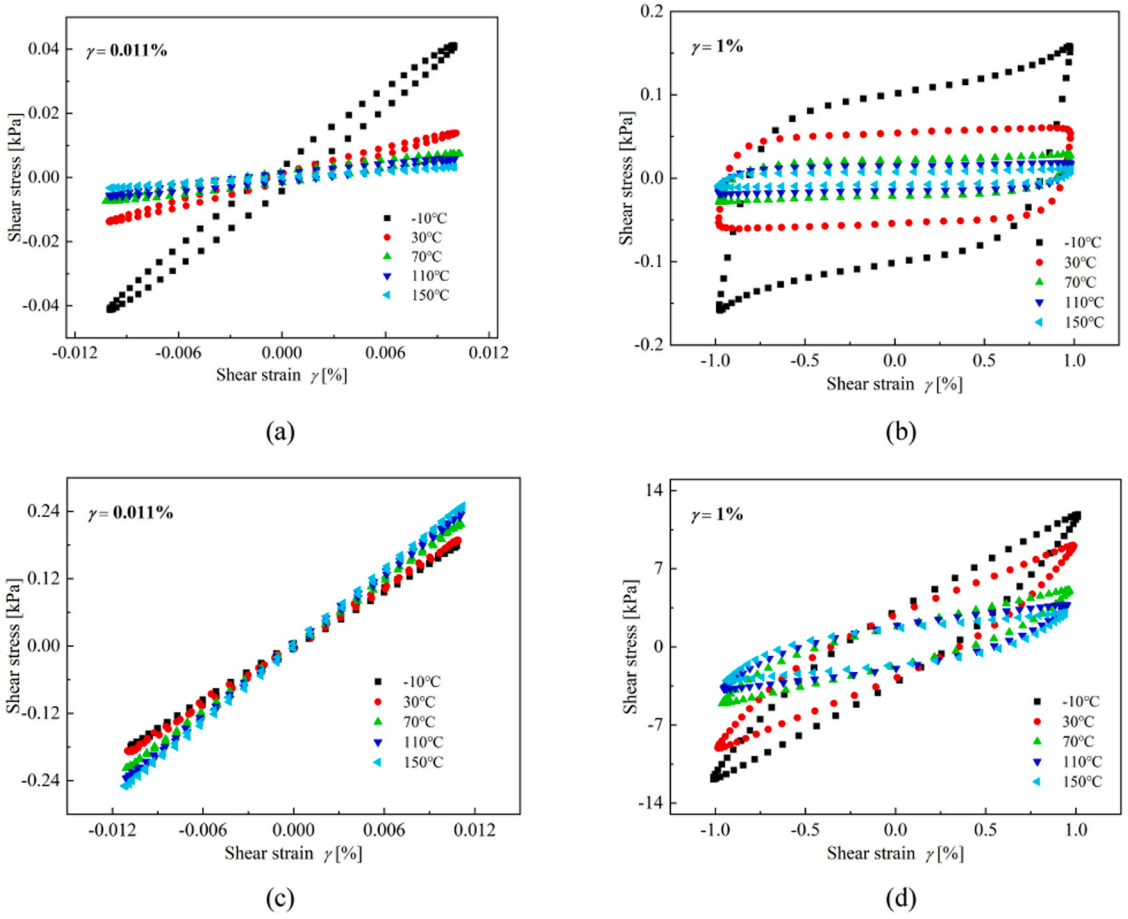

Fig. 3. The influence of the temperature on the stress-strain hysteresis loops of MR grease subject to small/large strain amplitude and with/without magentic field. The excitation frequency is kept as 1 Hz. (a)0.011%,0mT; (b)1%,0mT; (c)0.011%,480mT; (d)1%,480mT.

fixed strain amplitude and magnetic field, temperature has almost no effect on the shape of the hysteresis curve. However, interestingly, at low strain amplitudes, i.e.,0.01%, the hysteresis loop slope exhibits a decrease with rising temperature under zero magnetic field, implying thermal-softening. In contrast, upon the application of a magnetic field, the slope displays a completely opposite trend with increasing temperature, indicating thermo-stiffening. This temperature dependence of the hysteresis loop slope stands in stark contrast to that of MR elastomers featuring a solid matrix [35,36]. Furthermore, after the strain amplitude increased into the nonlinear range, i.e,1%, plastic deformation occurs in MR grease. At this point, the slope of the hysteresis curve always decreases with increasing temperature, regardless of the presence or absence of a magnetic field.

Fig. 4(a)-(d) illustrate the variations of the storage and loss modulus with respect to shear strain amplitude under different temperatures and magnetic fields. It is evident that the linear viscoelastic range (LVE) of the MR grease continuously expands as the magnetic field intensity increases from 0 to 480 mT, i.e., from 0.007% to 0.03%, and the temperature has minimal effect on that LVE range, which is in contrast to the decrease in the LVE range of MR fluid with the increase in magnetic field [21,37]. In the LVE regime, it has been observed that the storage modulus exhibits a decreasing trend with increasing temperature under zero magnetic field. However, under the influence of a magnetic field, the storage modulus demonstrates an increasing trend with rising temperature, which is in line with the previously reported findings in the literature [5,32,33]. The temperature-dependent changes in the loss modulus exhibit a reduction with increasing magnetic field within the LVE range. However, unlike the storage modulus, the loss modulus is almost independent of temperature when the magnetic field intensity exceeds 240mT, which is attributed to the dominant role of elastic deformation of particle chain structure.

Furthermore, it is notable that the impact of temperature on the storage modulus in LVE range diminishes progressively as a magnetic field is applied. Specifically, when the magnetic field is not applied, the storage modulus undergoes a 66.7% change within the temperature range of −10℃ to 150℃, whereas at 480mT, the rate of change is reduced to 33.5%. This is because the soap fibers in the grease matrix are more susceptible to temperature effects than the magnetic-induced particle chain structure, and the higher the magnetic field, the greater the contribution of the strength of the magnetic particle chain structure to the storage modulus of MR grease. In summary, the LVE range increases with the rise of the magnetic field and is minimally influenced by temperature. Within the LVE range, the storage modulus and loss decreases with increasing temperature in the absence of a magnetic field, while it increases with temperature in the presence of a magnetic field. As the magnetic field increases, the influence of temperature on the storage modulus and loss modulus gradually diminishes.

As the strain amplitude surpasses the LVE regime, the storage modulus becomes non-constant with increasing strain amplitude, regardless of the presence of a magnetic field, the effect of temperature on the storage modulus gradually reduces. Once the strain amplitude exceeds 1%, the temperature's impact on the storage modulus can be considered insignificant which means that the magnetic particle chain is completely destroyed. The loss modulus demonstrates a peak value at different temperatures, and in the absence of a magnetic field, the peak value of the loss modulus decreases with temperature. Conversely, when the magnetic field is applied, the peak value of the loss modulus increases with temperature. The reason for above phenomenon is that in

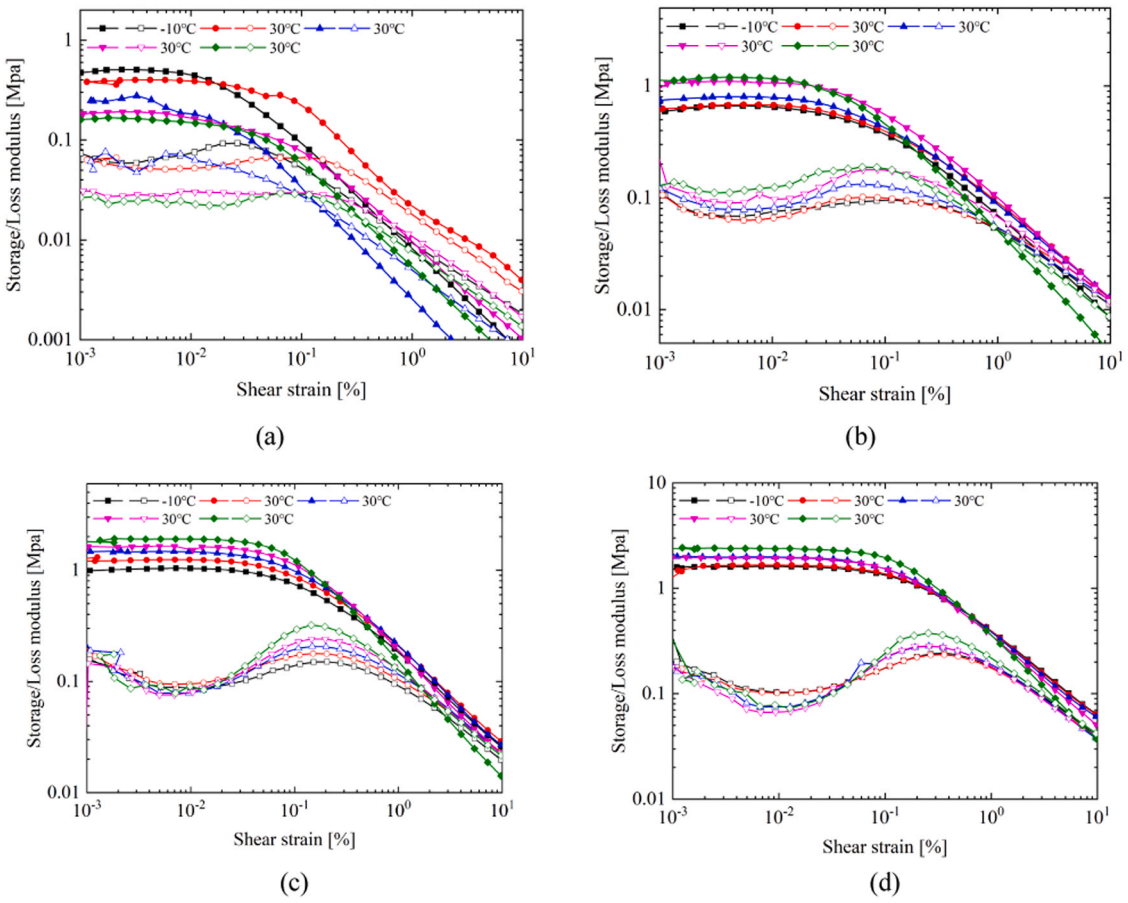

Fig. 4. The impact of temperature on the storage/loss modulus of MR grease at different strain amplitude and levels of magnetic flux density: (a)0mT; (b)120mT;(c) 240mT;(d)480mT. The excitation frequency is kept as 1 Hz. Closed symbols denote storage modulus and open symbols denote loss modulus.

the absence of a magnetic field, the energy dissipation in MR grease under large strain shear primarily arises from the destruction of entangled soap fibers within the grease matrix, with these fibers being more susceptible to breakage at higher temperatures. However, in the presence of a magnetic field, the energy dissipation mainly comes from the breakage of CIPs structure. At high temperatures, the degree of entanglement of the lubricating grease is reduced, which weakens its influence on the arrangement of CIPs and thus forms more difficult-to-break magnetized particle chains. As the strain amplitude increases further, regardless of the presence of a magnetic field, the soap fiber or particle chain structure is completely destroyed, and the effect of temperature on the energy dissipation modulus can be almost ignored.

4.3. Temperature dependent magneto-dynamic behavior under different oscillation frequency

The temperature dependence of stress-strain hysteresis loops for MR grease under different frequencies, i.e.,0.1 Hz and 5 Hz, and magnetic fields, i.e.,0 mT, 240 mT and 480 mT, are shown in Fig. 5. The excitation strain amplitude is kept as 1%. It can be observed that, at a constant magnetic field, the shape of the stress-strain hysteresis curves at different frequencies exhibits a similar trend with temperature, indicating that the influence of frequency on temperature-related stress-strain hysteresis curves is limited. In addition, at a constant frequency, regardless of the presence or absence of a magnetic field, the slope of the hysteresis curve exhibits a pattern of initially rapid increase followed by a gradual leveling off with increasing temperature.

To further describe the frequency-dependent dynamic performance of MR grease at different temperatures, Fig. 6 presents the variation of storage and loss modulus with frequency in the temperatures range from −10 ℃ to 150℃. Storage modulus and loss modulus of MR grease under different magnetic fields vary almost consistently with frequency, which aligns closely with the MR fluid behavior reported by Vicente et al. [22]. Furthermore, it is evident that the storage modulus at varying temperatures exhibits an almost invariant nature as the excitation frequency is heightened, similar phenomena also appear in literature [30,31,33], indicating the relative stability characteristics of the microstructure of MR grease. On the other hand, the temperature sensitivity of the storage modulus for MR grease diminishes as the external magnetic field escalates. Specifically, as the magnetic field strength surges from 0 mT to 480 mT, the rate of variation of the storage modulus within the temperature range of −10 ℃ to 150℃ at a frequency of 100 Hz diminishes from 55.5% to 5%, which suggests that the effect of temperature on the energy stored due to shear strain decreases as the magnetic field strength increases [30].

By comparing the storage modulus and loss modulus shown in Fig. 6, it can be seen that the loss modulus is much smaller than the storage modulus, indicating the solid-like behavior of MR grease. When the magnetic field is not applied, the loss modulus remains almost constant with increasing frequency, followed by a slight increase. However, in the presence of a magnetic field, the loss modulus decreases slightly with increasing frequency initially and then increases slightly. Moreover, it is noteworthy that, for a given frequency, the loss modulus exhibits remarkable variations with temperature under different magnetic field strengths. Specifically, at zero magnetic field intensity, the energy dissipation modulus decreases as the temperature increases, while at a magnetic field intensity of 120 mT, the energy dissipation modulus increases as the temperature increases. Intriguingly, when the magnetic field intensity is raised to 240 mT, the energy dissipation modulus shows a reversal and decreases again with increasing temperature, a

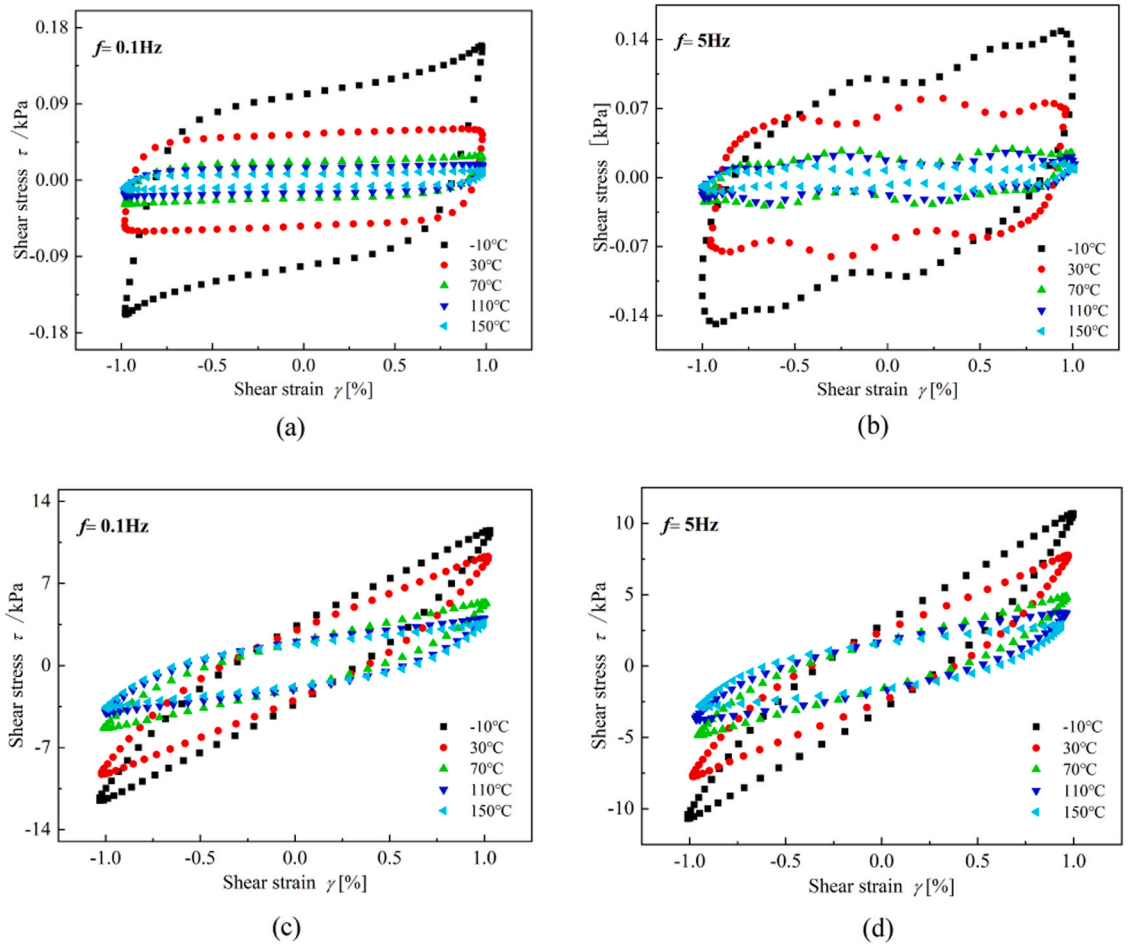

Fig. 5. The influence of the temperature on the stress-strain hysteresis loops of MR grease subject to different frequency and magnetic field. The excitation strain amplitude is kept as 1%. (a)0.1 Hz, 0mT;(b) 5 Hz, 0mT; (c)0.1 Hz, 480mT; (d)5 Hz, 480mT;.

phenomenon which has not been observed in prior investigations [5, 37]. The underlying reasons for this intriguing behavior will be elaborated in detail later in Section 4.4.

4.4. Temperature dependent dynamic behavior under magnetic field sweep in LVE range

In order to further investigate the interplay between the temperature dependence of the dynamic behavior of MR grease and their magnetic flux intensity, Fig. 7 illustrates the variation of the linear storage/loss modulus with magnetic field strength in the temperature range of −10℃ to 150℃. With the elevation of the magnetic field, the storage modulus demonstrates a sustained initial ascent, reaching a saturation point, whereas the loss modulus undergoes an initial increment followed by a subsequent decrement. Table 3 demonstrates the initial storage modulus, maximum magneto-induced modulus and maximum MR effect of MR grease under different temperature. It can be observed that the initial storage modulus decreases as the temperature rises, whereas the maximum magneto-induced modulus shows an increase with rising temperature. When the temperature increases from −10℃ to 150℃, the maximum magneto-induced modulus increases from 1465 KPa to 2029 KPa, which is almost 38% increase. Furthermore, the MR effect of the MR grease at −10℃ and 150℃ exhibit a difference of almost three times, with 360% and 1302% respectively. The substantial variation highlights the significant influence of temperature on the MR effect, emphasizing the need for establishing appropriate compensating mechanisms during device design of MR grease.

An intriguing observation in Fig. 7 involves the storage modulus and loss modulus, each manifesting a critical magnetic field, i.e., 100 mT and 270 mT respectively, that induces a diametrically opposite temperature-dependent response. Similar phenomena have not been observed previously within a relatively narrow temperature range [30,33,36].To better explain the mechanism of the changes in the storage modulus and loss modulus in Fig. 7, Fig. 8 provides a schematic of the temperature dependence of the microstructure of MR grease under three types of magnetic fields, i.e., zero-field, low magnetic field and high magnetic field. As known, storage modulus represents the deformation energy stored by the sample during the shear process, and for MR grease, it is mainly determined by the coupling interaction between the highly entangled soap fiber structure of grease matrix and CIPs chain structures induced by the magnetic field. At low magnetic field, the formation of chain structures by CIPs is limited due to the binding of soap fibers (as shown in Fig. 8(b)). At this juncture, the storage modulus is predominantly dictated by the lubricating grease matrix. The higher the temperature, the lower the degree of entanglement of the soap fibers (as depicted in Fig. 8(e)), which results in a smaller storage modulus. Ultimately, as shown in Fig. 7(a), the storage modulus decreases with increasing temperature when the magnetic field strength is below 100 mT. However, when the magnetic field exceeds the critical value, i.e., 100 mT, the augmented magnetic driving force can surmount the confines of soap fibers, enabling CIPs to align themselves into chain structures, and thereby causing the storage modulus to be primarily determined by the strength of the CIPs chain structures (as depicted in Fig. 8(c)). Moreover, as the temperature increases, the degree of soap fiber entanglement decreases, thereby reducing the hindrance to the formation of CIPs into chain structure. As a result, the strength of CIPs

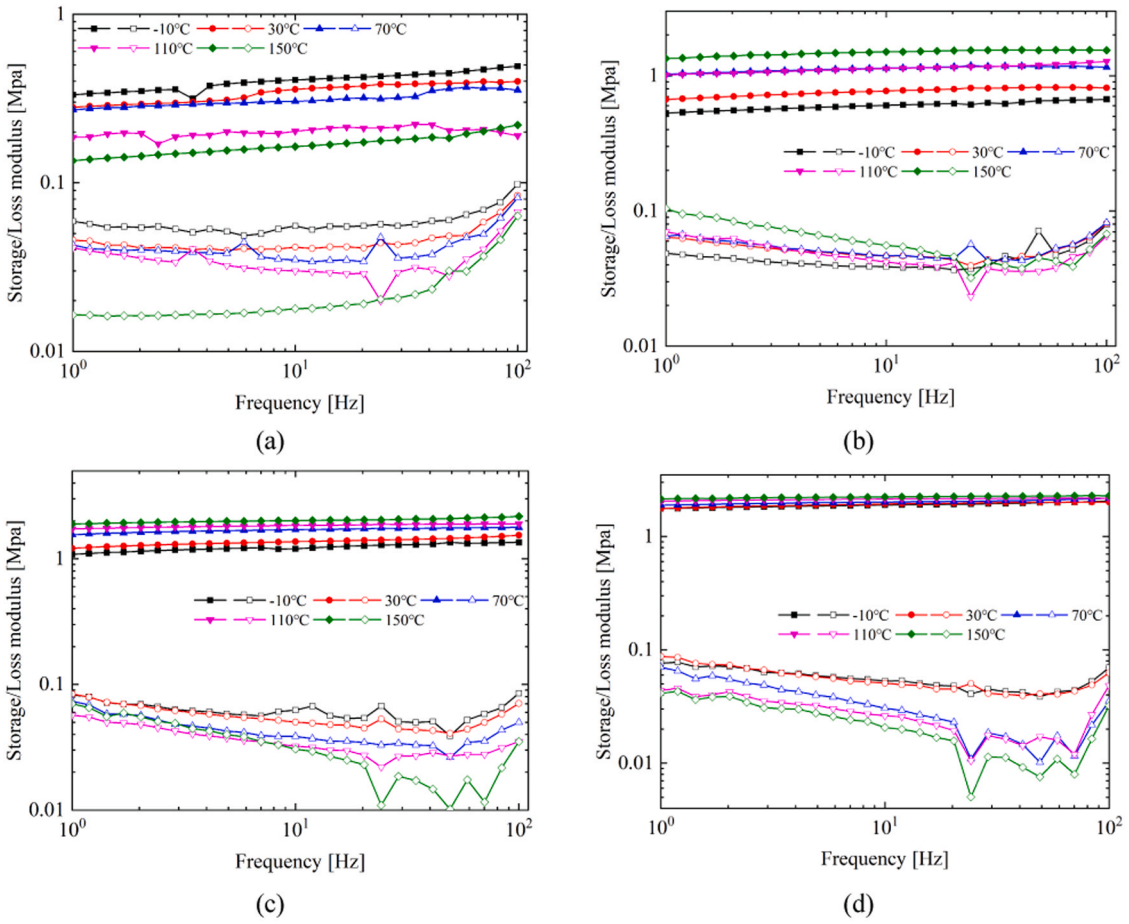

Fig. 6. The temperature dependence of storage and loss modulus for MR grease under different excitation frequency at various magnetic field: (a) 0mT; (b)120mT; (c) 240mT; (d) 480mT. The strain amplitude is fixed as 0.01%. Closed symbols denote storage modulus and open symbols denote loss modulus.

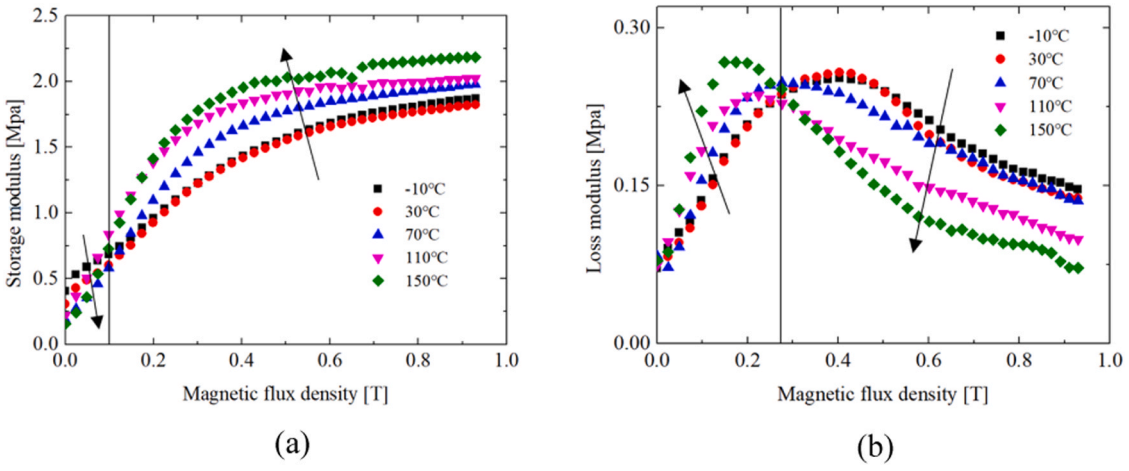

Fig. 7. Effect of temperature on the linear storage and loss modulus of MR grease in the magnetic flux density range of 0–960 mT : (a) storage modulus, (b)loss modulus. The strain amplitude and frequency are fixed as 0.01% and 1 Hz, respectively.

chain structure increases (as shown in Fig. 8(c) and (f)), which is the reason why the storage modulus increases with the increase of temperature in Fig. 7(a) when the magnetic field strength exceeds 100 mT.

Loss modulus represents the energy dissipated as heat during cyclic deformation of a material [23]. One possible explanation for the trend observed in Fig. 7(b) is as follows: At low magnetic field, the CIPs in the MR grease cannot form healthy long-chain structures due to the constraints of the soap fibers, and at higher temperatures, more of these unhealthy short-chain structures are formed (as shown in Fig. 8(e)), thus leading to an increase in loss modulus with increasing temperature. As the magnetic field increases beyond 270 mT, the CIPs chain structures become more stable and resistant to destruction (as illustrated in Fig. 8 (c)). In this case, the loss modulus primarily arises from friction between the chain structures and the MR grease matrix (the chain structures itself only undergo elastic deformation in this case), and as temperature increases, the degree of soap fiber entanglement decreases, thereby

Table 3
The initial storage modulus, maximum magneto-induced modulus and maximum MR effect of MR grease under different temperatures.

Temperature T (℃)	Initial storage modulus $G_0^{'}(KPa)$	Maximum magneto-induced modulus $\Delta G_{max}^{'}(KPa)$	Maximum MR effect $(\Delta G_{max}^{'}/G_0^{'}) \times 100\%$
-10	406	1465	360%
30	308	1517	493%
70	186	1792	961%
110	223	1802	806%
150	155	2029	1302%

reducing the friction between the chain structures and the MRG matrix (as illustrated in Fig. 8(f)), resulting in a decrease in energy dissipation modulus with increasing temperature, as observed in Fig. 7(b).

From the above discussion, it is evident that the configuration of the hysteresis loop in MR grease is markedly affected by the strain amplitude and magnetic field strength, while being comparatively less responsive to changes in temperature and oscillation frequency. The sensitivity of the storage/loss modulus is pronounced with respect to strain amplitude, magnetic field, and temperature, while exhibiting a relatively low sensitivity to frequency. The aforementioned characteristics of MR grease differ from traditional MR materials, such as MR fluid and elastomers. In the case of MR fluid, Masoud et al. found that the influence of temperature on storage modulus gradually decreases with the application of magnetic field, the loss modulus also decreases with increase in the temperature and it remains almost constant for higher temperatures [38]. In the case of MR elastomers, Xu et al. indicated that the storage modulus of MR elastomers becomes larger for increasing magnetic field and decreases when increasing the temperature. The loss modulus decreases with increasing magnetic field and hardly changes when increasing temperatures [39]. Zhang et al. presented that storage modulus of MREs with different proportions of matrix all showed a tendency of decreasing with the increase of temperature [40]. Wang et al. showed that the storage modulus decreased rapidly with increasing temperature. The loss modulus decreases linearly from the maximum value with increasing temperature and stabilizes gradually around 60°C. And the temperature characteristics are more sensitive with increasing magnetic field [36]. In the above literature, MREs and MR fluid all show that the modulus increases with increasing magnetic field, which is consistent with the MR grease in this manuscript. Furthermore, MREs and MR fluid also show a consistent trend with temperature, i.e., both storage and loss modulus decrease with increasing temperature, regardless of the presence or absence of a magnetic field. However, the MR grease shows that the storage modulus decreases with increasing temperature in the absence of a magnetic field, but increases with temperature in the presence of a magnetic field. Conversely, for the loss modulus, it exhibits a completely opposite phenomenon due to the influence of unique soap fiber structure of the grease matrix.

5. Magnetic field- and temperature-dependent dynamic shear modulus model

In order to verify the effectiveness of the proposed model for magnetic field- and temperature- dependent storage and loss modulus, Eq. (A25) was utilized to fit the experimental data from the previous sections with an oscillatory frequency of 1 Hz and a strain amplitude of 0.01%, and the fitted parameters are presented in Table 4. Fig. 9 shows the comparison between the simulated storage and loss modulus obtained from Eq. (A25) and the experimentally data. It can be seen that the proposed model can describe the storage modulus well, but the accuracy of describing the energy dissipation modulus is slightly lower. Overall, the proposed five-parameter model can predict the storage and loss modulus of MR grease under different temperatures and magnetic fields, indicating the effectiveness of the model.

Table 4
the constants for the proposed model of magnetic field- and temperature-dependent storage and loss modulus of MR grease.

Constants	Values
a_1, a_2, a_3, a_4, a_5	0.88, 1.28, −2.14, 1.23, 1.93,
a_6, a_7, a_8, a_9, a_{10}	3.25, −0.09, 2.21, 0.78, 17.4
a_{11}, a_{12}, a_{13}, a_{14}, a_{15}, b	1.26, −0.71,0.011, −0.0015, −1.08, −0.00164

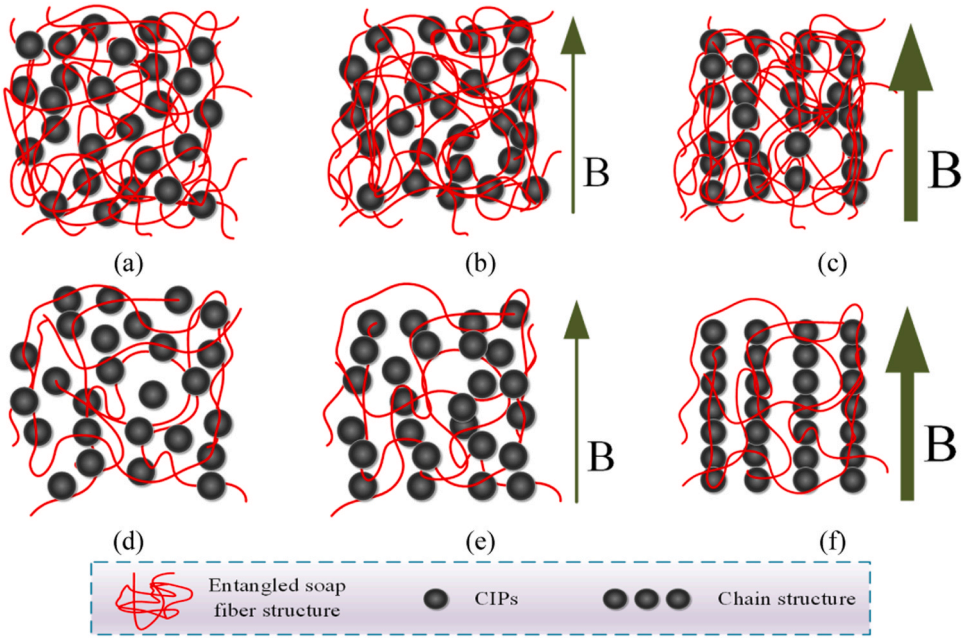

Fig. 8. Schematic diagram of the temperature dependent microstructure for MR grease under three types of magnetic field: (a)low temperature and without magnetic field;(b) low temperature and small magnetic field;(c) low temperature and large magnetic field;(d) high temperature and without magnetic field; (e) high temperature and small magnetic field;(f) high temperature and large magnetic field.

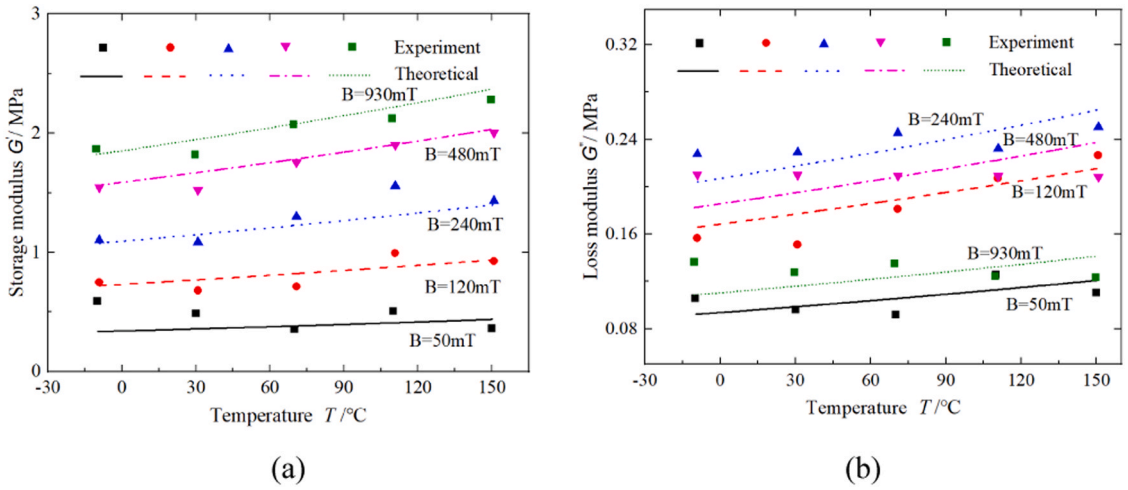

Fig. 9. Comparison of experimental and theoretical calculations of the storage/loss modulus of MR grease under different temperature and magnetic field.

6. Conclusion

An experimental and modeling study was conducted to investigate the dynamic characteristics of MR grease, i.e., stress-strain hysteresis characteristics and storage/loss modulus variation, under different oscillatory strain amplitudes, frequencies, magnetic fields in a wide temperature range from −10 °C to 150°C. In the experiments of oscillatory strain amplitude and frequency sweep, the shape of the hysteresis loop for MR grease is significantly influenced by the strain amplitude and magnetic field intensity, but is relatively insensitive to temperature and oscillation frequency. In the absence of a magnetic field, MR grease exhibits a thermal-softening effect. However, when the magnetic field is applied, MR grease demonstrates thermo-stiffening behavior with increasing temperature. On the other hand, the storage/loss modulus is highly sensitive to the strain amplitude, magnetic field, and temperature, but relatively insensitive to frequency. The influence of temperature on the storage modulus and loss modulus exhibits completely opposite characteristics in the absence and presence of a magnetic field. Additionally, with the increase in magnetic field, the impact of temperature on both the storage modulus and loss modulus gradually diminishes, i.e., when the magnetic field is not applied, the storage modulus undergoes a 66.7% change within the temperature range of −10 ℃ to 150℃, whereas at 480mT, the rate of change is reduced to 33.5%. In the magnetic field sweep experiments, the identification of a critical magnetic field, specifically at 100 mT for the storage modulus and 270 mT for the loss modulus, revealed a remarkably divergent temperature-dependent behavior observed both before and after surpassing this critical threshold. Finally, A model consisting of a five-parameter viscoelastic model and Arrhenius equation was proposed to predict the magnetic field- and temperature-dependent storage/loss modulus of MR grease under different oscillatory strain amplitude and frequency, and the effectiveness of the model was verified by comparing experimental and simulated results. The above-mentioned results lay the foundation for comprehending the magnetothermal coupling mechanism of MR grease and for the subsequent design of related devices.

CRediT authorship contribution statement

Wang Jiong: Writing – original draft. **Li Yancheng:** Writing – review & editing. **Xue Shuna:** Writing – original draft. **Qian Kun:** Writing – original draft. **Wang Huixing:** Writing – original draft.

Declaration of Competing Interest

The authors declare that they have no known competing financial interests or personal relationships that could have appeared to influence the work reported in this paper.

Data availability

Data will be made available on request.

Acknowledgments

This work has been supported by the China National Natural Science Foundation (No.52075264), China Postdoctoral Science Foundation (No. 2022M711621), and Jiangsu Natural Science Foundation (BK20230926).

Appendix

To better understand the above-mentioned dynamic behavior of MR grease in response to changing magnetic fields and temperatures at various oscillatory shear, a five-parameter model consisting of two Maxwell units and a spring connected in parallel, as illustrated in Figure A1, is proposed. The above three units can be represented as [41]:

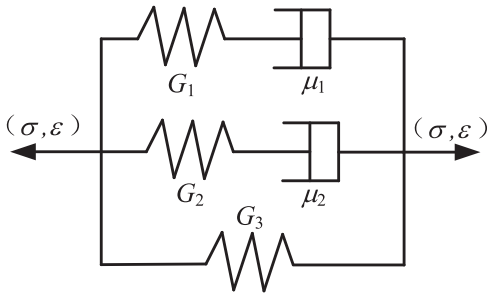

Fig. A1. The proposed dynamic shear modulus of MR grease consisting of two Maxwell units and a spring connected in parallel.

$$\sigma_1 = G_1\gamma_1 = \mu_1(\dot{\varepsilon}_1 - \dot{\gamma}_1) \tag{A1}$$

$$\sigma_2 = G_2\gamma_2 = \mu_2(\dot{\varepsilon}_2 - \dot{\gamma}_2) \tag{A2}$$

$$\sigma_3 = G_3\gamma_3 = G_3\varepsilon_3 \tag{A3}$$

The total stress and strain are:

$$\sigma = \sigma_1 + \sigma_2 + \sigma_3 \tag{A4}$$

$$\varepsilon = \varepsilon_1 = \varepsilon_2 = \varepsilon_3 \tag{A5}$$

To obtain the standard constitutive relation, Laplace transform is performed on Eqs. (A1), (A2), and (A3), yielding:

$$\overline{\sigma}_1 = G_1\overline{\gamma}_1 = \mu_1(s\overline{\varepsilon}_1 - s\overline{\gamma}_1) \tag{A6}$$

$$\overline{\sigma}_2 = G_2\overline{\gamma}_2 = \mu_2(s\overline{\varepsilon}_2 - s\overline{\gamma}_2) \tag{A7}$$

$$\overline{\sigma}_3 = G_3\overline{\varepsilon}_3 \tag{A8}$$

Substituting Eqs. (A5), (A6), (A7), and (A8) into Eq. (A4), we obtain:

$$G_1\frac{\mu_1 s}{G_1 + \mu_1 s} + G_2\frac{\mu_2 s}{G_2 + \mu_2 s} + G_3\overline{\varepsilon} = \overline{\sigma} \tag{A9}$$

After performing inverse Laplace transform, the standard constitutive expression is obtained as follows:

$$p_0\sigma + p_1\dot{\sigma} + p_2\ddot{\sigma} = q_0\varepsilon + q_1\dot{\varepsilon} + q_2\ddot{\varepsilon} \tag{A10}$$

where:

$$\begin{aligned} p_0 &= 1; \\ p_1 &= \left(\frac{\mu_1}{G_1} + \frac{\mu_2}{G_2}\right); \\ p_2 &= \left(\frac{\mu_1\mu_2}{G_1G_2}\right); \\ q_0 &= G_3; \\ q_1 &= \left(\mu_1 + \mu_2 + \frac{\mu_1}{G_1}G_3 + \frac{\mu_2}{G_2}G_3\right); \\ q_2 &= \left(\frac{\mu_1\mu_2}{G_1} + \frac{\mu_1\mu_2}{G_2} + \frac{\mu_1\mu_2}{G_1G_2}G_3\right); \end{aligned} \tag{A11}$$

In the linear viscoelastic range, when a sinusoidal strain excitation, i.e.,$\varepsilon(t) = \varepsilon_0 e^{i\omega t}$, is applied to the MR grease, the stress response is given by:

$$\sigma(t) = \sigma^* e^{i\omega t} \tag{A12}$$

In the equation:

$$\sigma^* = \varepsilon_0 G^*(i\omega) \tag{A13}$$

Where:

$$G^*(i\omega) = G'(i\omega) + iG''(i\omega) \tag{A14}$$

To obtain the storage modulus and loss modulus in (A14), the Eq. (A10) is rewritten as:

$$P\sigma = Q\varepsilon \tag{A15}$$

The differential operator in the Eq. (A15) is

$$P = \sum_{k=0}^{m} p_k \frac{d^k}{dt^k}$$
$$Q = \sum_{k=0}^{n} q_k \frac{d^k}{dt^k} \tag{A16}$$

Substituting $\varepsilon(t) = \varepsilon_0 e^{i\omega t}$ into the right-hand side of Eq. (A15), we obtain:

$$\sum_{k=0}^{m} p_k \frac{d^k \sigma}{dt^k} = \sum_{k=0}^{n} q_k (i\omega)^k \varepsilon_0 e^{i\omega t} \tag{A17}$$

Thus, the stress response, i.e.,σ(t), can be obtained from Eqs. (A12), (A15)-(A17) as follows:

$$\sigma(t) = \frac{Q(i\omega)}{P(i\omega)} \varepsilon_0 e^{i\omega t} \tag{A18}$$

Where the operator in the Eq. (A18) is:

$$P\left(i\omega\right) = \sum_{k=0}^{m} p_k (i\omega)^k$$
$$Q\left(i\omega\right) = \sum_{k=0}^{n} q_k (i\omega)^k \tag{A19}$$

Thus, the complex modulus in Eq. (A14) is:

$$G^*\left(i\omega\right) = \frac{Q(i\omega)}{P(i\omega)} \tag{A20}$$

The storage modulus and loss modulus under sinusoidal strain excitation can be obtained from Eq. (A20) as:

$$G'(f) = G_3 + G_1 \frac{(2\pi f \tau_1)^2}{1 + (2\pi f \tau_1)^2} + G_2 \frac{(2\pi f \tau_2)^2}{1 + (2\pi f \tau_2)^2}$$
$$G''(f) = G_1 \frac{(2\pi f \tau_1)}{1 + (2\pi f \tau_1)^2} + G_2 \frac{(2\pi f \tau_2)}{1 + (2\pi f \tau_2)^2} \tag{A21}$$

Where:

$$\tau_1 = \frac{\mu_1}{G_1}, \tau_2 = \frac{\mu_2}{G_2} \tag{A22}$$

To establish the relationship between the storage/loss modulus and the magnetic field, the relationships between the parameters in Eq. (A21) and the magnetic field are established as follows:

$$\tau_1 = \frac{1}{(a_1 + a_2 B)^{a_3}}, \tau_2 = \frac{1}{(a_4 + a_5 B)^{a_6}}, G_1 = (a_7 + a_8 B)^{a_9},$$
$$G_2 = (a_{10} + a_{11} B)^{a_{12}}, G_3 = a_{13} + \frac{(a_{11} B)^2}{1 + (a_{15} B)} \tag{A23}$$

On the other hand, to detect the relationship between the storage/loss modulus of MR grease and temperature, a commonly used Arrhenius equation is introduced here [42]:

$$\eta = A\exp(E_a / RT) \tag{A24}$$

Where R is the gas constant, Ea is the activation energy and A is the constant coefficient.

Inspired by the temperature-dependent yield stress model of MR materials employing Arrhenius equation in previous literature [43-45], and in conjunction with the magnetic field-dependent storage/loss modulus model presented above, we finally propose the magnetic field- and temperature-dependent storage and loss modulus model for MR grease as follows:

$$G'\left(B,T\right) = \left(G_3 + G_1 \frac{(2\pi f \tau_1(B))^2}{1 + (2\pi f \tau_1(B))^2} + G_2 \frac{(2\pi f \tau_2(B))^2}{1 + (2\pi f \tau_2(B))^2}\right) * e^{-bT}$$
$$G''\left(B,T\right) = \left(G_1 \frac{(2\pi f \tau_1(B))}{1 + (2\pi f \tau_1(B))^2} + G_2 \frac{(2\pi f \tau_2(B))}{1 + (2\pi f \tau_2(B))^2}\right) * e^{-bT} \tag{A25}$$

Appendix A. Supporting information

Supplementary data associated with this article can be found in the online version at doi:10.1016/j.colsurfa.2024.133468.

References

[1] R.F. Gibson, A review of recent research on mechanics of multifunctional composite materials and structures, Compos. Struct. 92 (12) (2011) 2793–2810.
[2] R. Ahamed, S.B. Choi, M.M. Ferdaus, A state of art on magneto-rheological materials and their potential applications, J. Intell. Mater. Syst. Struct. 29 (10) (2018) 2051–2095.
[3] N. Mohamad, S.A. Mazlan, S.B. Choi, et al., The field-dependent rheological properties of magnetorheological grease based on carbonyl-iron-particles, Smart Mater. Struct. 25 (9) (2016) 095043.
[4] A.K. Bastola, M. Hossain, A review on magneto-mechanical characterizations of magnetorheological elastomers, Compos. Part B: Eng. 200 (2020) 108348.
[5] H.X. Wang, Y.C. Li, G. Zhang, et al., Effect of temperature on rheological properties of lithium-based magnetorheological grease, Smart Mater. Struct. 28 (3) (2019) 035002.
[6] Aashna Raj, et al., Investigation of magnetorheological grease flow under the influence of a magnetic field, J. Mol. Liq. 361 (2022) 119682.
[7] S. Tarmizi, N.A. Nordin, S.A. Mazlan, et al., Improvement of rheological and transient response of magnetorheological grease with amalgamation of cobalt ferrite, J. Mater. Res. Technol. (2022).
[8] M.A. Aziz, S.M. Mohtasim, R. Ahammed, State-of-the-art recent developments of large magnetorheological (MR) dampers: a review, Korea-Aust. Rheol. J. 34 (2) (2022) 105–136.
[9] S.J. Dyke, J.B.F. Spencer, M.K. Sain, J.D. Carlson, Modeling and control of magnetorheological dampers for seismic response reduction, Smart Mater. Struct. 5 (5) (1996) 565.
[10] I.I.M. Yazid, S.A. Mazlan, T. Kikuchi, H. Zamzuri, F. Imaduddin, Design of magnetorheological damper with a combination of shear and squeeze modes, Mater. Des. 54 (2014) 87–95.
[11] Y.C. Li, J.C. Li, W.H. Li, H.P. Du, A state-of-the-art review on magnetorheological elastomer devices, Smart Mater. Struct. 23 (12) (2014) 123001.
[12] M. Behrooz, X. Wang, F. Gordaninejad, Modeling of a new semi-active/passive magnetorheological elastomer isolator, Smart Mater. Struct. 23 (4) (2014) 045013.
[13] W.H. Li, X.Z. Zhang, H.P. Du, Development and simulation evaluation of a magnetorheological elastomer isolator for seat vibration control, J. Intell. Mater. Syst. Struct. 23 (2012) 1041–1048.
[14] J. Fu, P.D. Li, G.Y. Liao, J.J. Lai, M. Yu, Development and dynamic characterization of a mixed mode magnetorheological elastomer isolator, IEEE Trans. Magn. 53 (2016) 1–4.
[15] T. Hu, S. Xuan, L. Ding, X. Gong, Stretchable and magneto-sensitive strain sensor based on silver nanowire-polyurethane sponge enhanced magnetorheological elastomer, Mater. Des. (2018).
[16] F. Eloy, G.F. Gomes, A.C. Ancelotti, S.S. da Cunha, A.J.F. Bombard, D. M. Junqueira, A numerical-experimental dynamic analysis of composite sandwich beam with magnetorheological elastomer honeycomb core, Compos. Struct. 209 (2019) 242–257.
[17] J.Z. Chen, W.H. Liao, Design, testing and control of a magnetorheological actuator for assistive knee braces, Smart Mater. Struct. 19 (2010) 035029.
[18] H. Böse, R. Rabindranath, J. Ehrlich, Soft magnetorheological elastomers as new actuators for valves, J. Intell. Mater. Syst. Struct. 23 (9) (2012) 989–994.
[19] S. Kashima, F. Miyasaka, K. Hirata, Novel soft actuator using magnetorheological elastomer, IEEE Trans. Magn. 48 (4) (2012) 1649–1652.
[20] L.J. Felicia, J. Philip, Effect of hydrophilic silica nanoparticles on the magnetorheological properties of ferrofluids: a study using opto-magnetorheometer, Langmuir 31 (11) (2015) 3343–3353.
[21] J. Philip, Magnetic nanofluids (Ferrofluids): recent advances, applications, challenges, and future directions. Colloid Interface Sci. 311 (2023) 102810.
[22] J.D. Vicente, D.J. Klingenbergb, R. Hidalgo-Alvareza, Magnetorheological fluids: a review, Soft Matter 7 (2011) 3701–3710.
[23] D.J. Vicente, M.T. López-López, J.D.G. Durán, A slender-body micromechanical model for viscoelasticity of magnetic colloids: comparison with preliminary experimental data, J. Colloid Interface Sci. 282 (1) (2005) 193–201.
[24] J.M. Ginder, L.C. Davis, L.D. Elie, Rheology of magnetorheological fluids: models and measurements, Int. J. Mod. Phys. 23 (24) (1996) 3293–3303.
[25] B.D. Chin, H.H. Winter, Field-induced gelation, yield stress, and fragility of an electro-rheological suspension, Rheol. Acta 41 (3) (2002) 265–275.
[26] Mark R.J. Carlson, J.D. Munoz BC, A model of the behaviour of magnetorheological materials, Smart Mater. Struct. 5 (1996) 607–614.
[27] N. Mohamad, S.A. Mazlan, F. Imaduddin, S.B. Choi, I.I.M. Yazid, A comparative work on the magnetic field-dependent properties of plate-like and spherical iron particle-based magnetorheological grease, PLOS One 13 (4) (2018) e0191795.
[28] N. Mohamad, S.A. Mazlan, S.B. Choi, et al., The effect of particle shapes on the field-dependent rheological properties of magnetorheological greases, Int. J. Mol. Sci. 20 (2019) 1525.
[29] S.M.A. Tarmizi, N.A. Nordin, S.A. Mazlan, et al., Improvement of Rheological and transient response of magnetorheological grease with amalgamation of cobalt ferrite, J. Mater. Res. Technol. (2022).
[30] H.X. Wang, T.X. Chang, Y.C. Li, S.Q. Li, et al., Characterization of nonlinear viscoelasticity of magnetorheological grease under large oscillatory shear by using Fourier transform-Chebyshev analysis, J. Intell. Mater. Syst. Struct. 32 (2021) 614–631.
[31] J.B. Pan, G.X. Yang, J.P. Wang, X.C. Wang, X.L. Wang, Thermorheological properties of magnetorheological grease and its thermomagnetic coupling mechanism, J. Intell. Mater. Syst. Struct. 33 (2022) 432–444.
[32] X.D. Ye, J. Wang, X.J. Wang, G. Zhang, Q. Ouyang, An experimental study on thermo-field rheological properties of lithium-based magnetorheological grease, Colloids Surf. A: Physicochem. Eng. Asp. 648 (2022) 129047.
[33] X.D. Ye, W.C. Wang, J. Wang, The influence of temperature on the rheological properties of composite lithium-based magnetorheological grease, J. Intell. Mater. Syst. Struct. 33 (2022) 2336–2345.
[34] B.O. Park, B.J. Park, M.J. Hato, H.J. Choi, Soft magnetic carbonyl iron microsphere dispersed in grease and its rheological characteristics under magnetic field, Colloid Polym. Sci. 289 (2011) 381–386.
[35] M. Hemmatian, R. Sedaghati, S. Rakheja, Characterization and modeling of temperature effect on the shear mode properties of magnetorheological elastomers, Smart Mater. Struct. 29 (11) (2020) 115001.
[36] Y. Wan, Y. Xiong, S. Zhang, Temperature dependent dynamic mechanical properties of magnetorheological elastomers: experiment and modeling, Compos. Struct. 202 (2018) 768–773.
[37] S.S. Deshmukh, H.M. GarethRheological behavior of magnetorheological suspensions under shear, creep and large amplitude oscillatory shear (LAOS) flow. In: Proceedings of the XIVth International Congress on Rheology, 8, pp. 22-27 2004, , 22–27..
[38] H. Masoud, R. Sedaghati, S. Rakheja, Temperature dependency of magnetorheological fluids' properties under varying strain amplitude and rate, J. Magn. Magn. Mater. 498 (2020) 166109.
[39] Y. Xu, X. Gong, S. Xuan, A high-performance magnetorheological material: preparation, characterization and magnetic-mechanic coupling properties, Soft Matter 7 (2011) 5246–5254.
[40] Y. Zhang, X. Gong, S. Xuan, Temperature-dependent mechanical properties and model of magnetorheological elastomers, Ind. Eng. Chem. Res. 50 (2011) 6704–6712.
[41] D. Fleisch, A Student's Guide to Maxwell's Equations, Cambridge University Press,, 2008.
[42] Keith J. Laidler, The development of the Arrhenius equation, J. Chem. Educ. 61 (1984) 494.
[43] R.S. Mao, G. Zhang, H.X. Wang, J. Wang, Temperature-dependent dynamic properties of magnetorheological gel composite: experiment and modeling, Smart Mater. Struct. 31 (2022) 035002.
[44] B. Yu, T. Keller, T. Vallée, Modeling of stiffness of FRP composites under elevated and high temperatures, Compos. Sci. Technol. 68 (2008) 3099–3106.
[45] B. Yu, N. Post, J. Lesko, T. Keller, Experimental investigations on temperature-dependent thermo-physical and mechanical properties of pultruded GFRP composites, Thermochim. Acta 469 (2008) 28–35.